ELSEVIER

Polymer 41 (2000) 5173–5184

polymer

Structure and properties of various poly(amic diisopropyl ester-*alt*-imide)s and their alternating copolyimides

S.I. Kim[a], T.J. Shin[a], M. Ree[a,*], H. Lee[a], T. Chang[a], C. Lee[b,1], T.H. Woo[b], S.B. Rhee[b]

[a]*Department of Chemistry and Polymer Research Institute, Pohang University of Science and Technology, San 31, Hyoja-dong, Pohang 790-784, South Korea*
[b]*Advanced Functional Polymers Group, Korea Research Institute of Chemical Technology, P.O. Box 9, Daedeog-danji, Yusung-gu, Taejon 305-606, South Korea*

Received 29 January 1999; received in revised form 4 October 1999; accepted 4 October 1999

Abstract

Several poly(amic diisopropyl ester-*alt*-imide)s have been synthesized, which are a new type of polyimide precursors. The precursors consist of amic ester and imide units alternatively on the backbone, so that they are hydrolytically stable as well as low shrinkable through thermal imidization. These precursors have an easy processability because of their good solubility in common solvents that are widely used as good solvents for most polyimide precursors. The precursors and their alternating copolyimides in films have exhibited structural orders that are estimated to have a dimension of 15–42 Å (along the chain axis) and 8–16 Å (along the lateral direction), depending upon the polymer backbone chemistry. However, all the precursors and resultant copolyimides were laterally packed in an irregular way. Their crystallinities were apparently low. These results might be attributed mainly to the bend or kinked units on the polymer backbone. In addition, properties of the precursors and their polyimides in films: optical and dielectric properties, glass transition, thermal imidization characteristics, thermal stability, thermal expansion and residual stress, were investigated in detail. Overall, the precursor polymers, as well as the resultant alternating copolyimides were characterized to have relatively good properties suitable for applications in the fabrication of microelectronic devices.

Keywords: Soluble poly(amic ester-*alt*-imide)s; Alternating copolyimides; Structure

1. Introduction

Aromatic polyimides are widely used in the microelectronics industry because of their excellent chemical and physical properties [1–4]. Most aromatic polyimides are insoluble and infusible [1,2]. The insolubility is mainly due to the aromatic and heterocyclic constituents on the polymer backbone [1,2]. And the infusibility is generally attributed to the high glass transition temperature (T_g) or high melting temperature (T_m) which is generated by the rigid aromatic and heterocyclic structures on the backbone [1,2]. Because of these problems, aromatic polyimides are always processed in soluble precursor polymers and then imidized chemically or thermally.

Poly(amic acid) can be easily synthesized in aprotic polar solvents, such as *N*-methyl-2-pyrrolidone, *N*,*N*-dimethylacetamide (DMAc) and *N*,*N*-dimethylformamide (DMF), from aromatic dianhydride and diamine, so that this polymer is widely used in the fabrication of microelectronic devices as the representative of polyimide precursors. However, poly(amic acid) is known to be in the equilibration with the constituent dianhydride and diamine [5,6]. Thus, molecular weight of the precursor polymer varies very sensitively with temperature variation and moisture contact, causing numerous problems in its quality control and process. In general, the precursor generally needs to stay in a refrigerator of <4°C to keep out of moisture contact in order to retain its molecular weight (or solution viscosity) in a proper level.

Another representative of polyimide precursor is poly(amic dialkyl ester). This precursor polymer is not in such monomer–polymer equilibration as observed for poly(amic acid), so that the precursor is hydrolytically stable [7–9]. Thus, poly(amic dialkyl ester) has gained great attention from academic and industry fields although its synthesis is relatively more complicate than that of poly(amic acid).

In applications, these precursor polymers in solvents are conventionally spin-cast and soft-baked. Finally, the soft-baked precursors in films are converted either chemically or

* Corresponding author. Tel.: + 82-562-279-2120; fax: +82-562-279-3399.
E-mail address: ree@postech.ac.kr (M. Ree).
[1] Co-corresponding author

0032-3861/00/$ - see front matter
PII: S0032-3861(99)00748-X

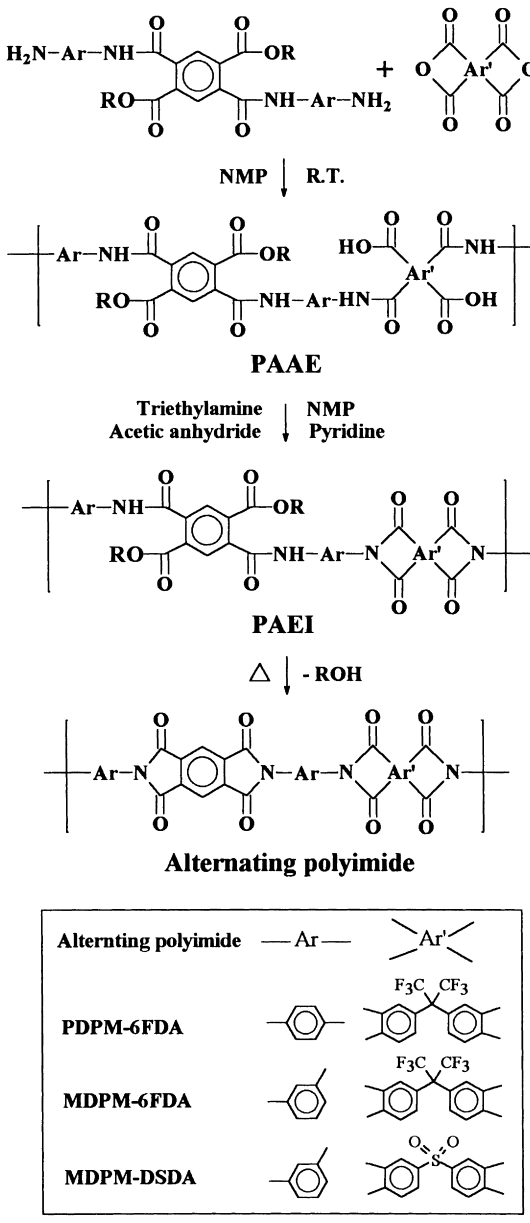

Fig. 1. Synthetic scheme of poly(amic diisopropyl ester-*alt*-imide) precursors and their alternating polyimides.

thermally to the polyimides. The thermal imidization process is widely employed particularly in the fabrication of microelectronic devices, compared to the chemical imidization process, because of its easy applicability. The thermal imidization is always accompanied with the removal of residual solvents and byproducts, leading to a significant shrinkage in volume. The chemical imidization is also accompanied by the removal of solvents and byproducts, causing large volume shrinkage. In general, both poly(amic acid) and poly(amic dialkyl ester) in soft-baked films are shrunk by approximately 50% through a conventional thermal imidization process [7–12]. The large shrinkage associated with the imidization processes sometimes causes serious problems on the fabrication process and resultant products: dimensional distortion, bending, curling and delamination. Thus, non-shrinkable or low shrinkable polyimide precursors are highly desired in the microelectronic industry.

In this study, there were synthesized a new type of polyimide precursors which are low shrinkable as well as hydrolytically stable. Three different poly(amic diisopropyl ester-*alt*-imide)s, which are the well-defined alternating copolymer precursors, were synthesized. Structures and properties of these precursor polymers and their copolyimides were investigated by X-ray diffraction, prism coupling, oscillating differential scanning calorimetry, thermogravimetry, thermomechanical analysis and residual stress analysis. The measured structures and properties were understood by considering the chemical structures and the imidization process.

2. Experimental

2.1. Synthesis

2,2′-Bis(3,4-dicarboxyphenyl)hexafluoropropane dianhydride (6FDA) and 3,3′,4,4′-diphenylsulfonetetracarboxylic dianhydride (DSDA) were supplied from Chriskev Company in Kansas, USA. Other chemicals used in this study were purchased from Aldrich Chemical Company (USA). DSDA and 6FDA were purified by recrystallization in acetic anhydride, respectively, followed by drying under reduced pressure. *N*-Methyl-2-pyrrolidone (NMP) was distilled over calcium hydride under reduced pressure.

Two different diamine monomers, *N*,*N*′-bis(4-aminophenyl)-2,5-(diisopropoxycarbonyl)benzene-1,4-dicarboxamide (PDPM) and *N*,*N*′-bis(3-aminophenyl)-2,5-(diisopropoxy-carbonyl)benzene-1,4-dicarboxamide (MDPM) were synthesized by methods reported previously [13,14].

Using these diamine monomers, three different poly(amic diisopropyl ester-*alt*-amic acid)s (PAAEs) were prepared from the polycondensation reactions with 6FDA and DSDA as follows. A poly(amic diisopropyl ester-*alt*-amic acid), PDPM–6FDA PAAE was prepared at room temperature by slowly adding the equimolar amount of the purified 6FDA to the PDPM in dry NMP (Fig. 1). Once the 6FDA addition was completed, the reaction flask was capped tightly and stirring was continued for two days at room temperature to make the polymerization mixture completely homogeneous. The other poly(amic diisopropyl ester-*alt*-amic acid)s, MDPM–6FDA PAAE and MDPM–DSDA PAAE, were prepared in the same manner as PDPM–6FDA PAAE (Fig. 1). Here, all the polymerizations were conducted in a glove box filled with dry nitrogen gas. For all the precursor solutions, the solid contents were about 10 wt.%.

These PAAE precursor polymers were converted to the corresponding poly(amic diisopropyl ester-*alt*-imide)s

(PAEIs) by the selective chemical imidization of amic acid units as follows. The selective imidization was carried out by the addition of acetic anhydride, triethylamine and pyridine to the PDPM–6FDA PAAE solution in NMP and stirred continuously for 2 h at 60°C. The reaction mixture was poured into a mixture of methanol and deionized water (1:1 in volume), and the precipitate was filtered, followed by washing with methanol several times. The obtained PDPM–6FDA PAEI polymer was dried for several days at 50°C under reduced pressure. The MDPM–6FDA and MDPM–DSDA PAEIs were prepared in the same manner as PDPM–6FDA PAEI (Fig. 1).

The synthesized PAAE precursors and their PAEIs were dissolved in dimethyl-d_6 sulfoxide (DMSO-d_6) and characterized using a Bruker NMR spectrometer (Model: Aspect 300 MHz) with a proton probe. The PDPM–6FDA and MDPM–6FDA PAEIs were identified by determining the chemical shifts of the aromatic protons of the 6FDA unit before and after the selective chemical imidization of their PAAE precursors. In the same manner, the MDPM–DSDA PAEI precursor was also identified by checking the chemical shifts of aromatic protons of the DSDA unit.

All the PAEI precursor polymers were soluble in NMP, DMSO, DMAc and DMF. For the synthesized PAEI precursor polymers, intrinsic viscosity $[\eta]$ measurements were carried out in NMP at 25.0°C using an Ubbelohde suspended level capillary viscometer. For a given PAEI precursor, the relative and specific viscosities were measured at four different concentrations over the range of 0.10–0.80 g/dl, and the $[\eta]$ value was estimated by extrapolation of the reduced and inherent viscosities to infinite dilution. The $[\eta]$ was determined to be 0.751 dl/g for the PDPM–6FDA PAEI, 0.480 dl/g for the MDPM–6FDA PAEI and 0.448 dl/g for the MDPM–DSDA PAEI.

2.2. Film preparation

The PAEI precursors were again dissolved in NMP and spin-cast on glass slides, followed by soft-baking on a hot plate at 80°C for 1 h. The soft-baked precursor films were dried further under reduced pressure in order to remove the residual solvent. The thickness of dried polymer films was 4–8 μm. Some of the dried polymer films were taken off from the glass substrates using deionized water, followed by drying for 1 day at 100°C in a vacuum oven. The films were cut in appropriate sizes for measurements of structures and properties. The other dried precursor films were thermally imidized in an oven with a dried nitrogen gas flow by a three-step imidization process: 150°C/30 min and 230°C/30 min at a ramping rate of 2.0 K/min and 380°C/1 h at a ramping rate of 5.0 K/min (Fig. 1). After the thermal imidization, the samples were cooled to room temperature at a rate of 10.0 K/min. The thickness of imidized films was 3–5 μm. The films were taken off from the glass substrates with the aid of deionized water, followed by drying for 1 day at 100°C in a vacuum oven. The imidized films were also used for the measurements of structures and properties.

In addition, PAEI precursor films were prepared for residual stress measurements as follows. Double-side polished Si (100) wafers (76 mm diameter and 380 μm thickness) have been adapted as substrates because their physical properties are well known. They were pre-cleaned with NMP using a spin-coater, followed by drying on a hot plate at 80°C for a few minutes in ambient air. γ-Aminopropyltriethoxysilane of 0.1 vol.% in deionized water, as an adhesion primer, was spin-applied on the Si wafers at 2000 rpm/20 s, and the wafers were dried at 115°C for 5 min in ambient air. Then, the PAEI precursor solutions were spin-coated on the primed Si wafers, followed by soft-baking at 80°C for 1 h. The soft-baked films were further dried under reduced pressure in order to remove the residual solvent.

2.3. Measurements

For fully dried PAEI precursor films, glass transition and imidization were investigated over 0–400°C using a Seiko oscillating differential scanning calorimeter (ODSC, Model 220CU) as described previously elsewhere [9,11,15]. During the measurement, dry nitrogen gas was purged with a flow rate of 80 ml/min, and temperature and enthalpy were calibrated using indium and tin, respectively. Film samples of ca. 2 mg were used. A heating rate of 10.0 K/min was employed. An oscillating amplitude of 10.0°C and an oscillating frequency of 0.02 Hz were used, respectively.

Wide angle X-ray diffraction (WAXD) measurements were performed at room temperature in both reflection and transmission geometry, using a Rigaku vertical diffractometer (Model RINT-2500) with an 18 kW rotating anode X-ray generator. The CuKα radiation source was operated at 40 kV and 60 mA. A divergence slit of 0.5° was employed together with a scattering slit of 0.5° and a receiving slit of 0.15 mm. All the measurements were carried in a $\theta/2\theta$ mode. The 2θ scan data were collected at 0.01° interval over the range of 4–60° and the scan speed was 0.1°(2θ)/min. WAXD patterns were corrected to the background runs and then deconvoluted as follows. An interactive curve-fitting technique based on a nonlinear-least-squares estimation algorithm was used to fit a collection of pseudo-Voight functions and one linear baseline to the WAXD profile was corrected as described previously [16,17]. For each deconvoluted peak, coherence length (L_C) was estimated from its full width at half-maximum (FWHM) with an instrumental broadening of 0.15° using the Scherrer equation: $L_C = \lambda/\text{FWHM} \cos\theta$ where λ and θ are the wavelength of X-ray radiation source used and the Bragg's angle of the peak, respectively [18,19].

Refractive indices were measured at room temperature using a prism coupler equipped with a He–Ne laser light source of 632.8 nm wavelength (that is, 474.08 THz in optical frequency) and controlled by a personal computer [18,20,21]. The refractive index in the film plane (n_{xy}) was

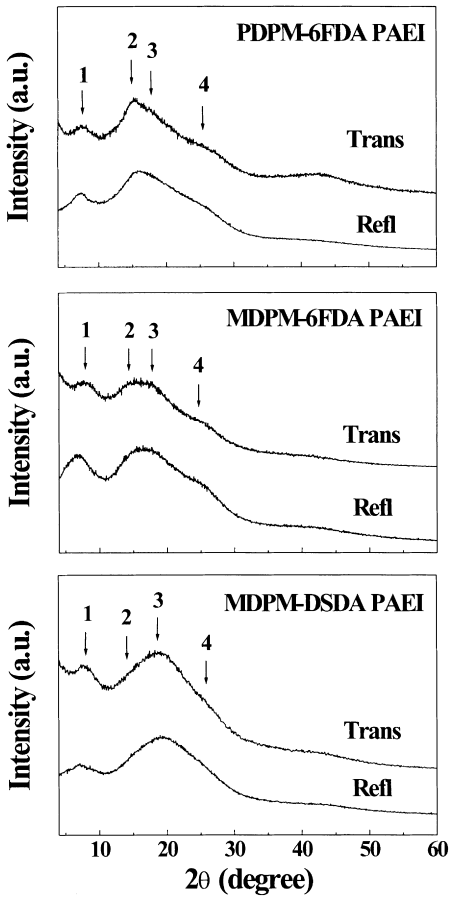

Fig. 2. Reflection and transmission X-ray diffraction patterns of poly(amic diisopropyl ester-*alt*-imide)s in films.

measured in the transverse electric mode, whereas the refractive index in the out-of-plane (n_z) was obtained in the transverse magnetic mode. All measurements were performed using a cubic zirconia prism of $n = 2.1677$ at a wavelength of 632.8 nm.

In-plane thermal expansion coefficients (TECs) were measured with a load of 5 g at a ramping rate of 5.0 K/min over the range of 50–250°C under dry nitrogen gas flow using a Seiko thermomechanical analyzer (TMA, Model 120CU) with a tension probe. For each sample run, the measured TECs were averaged out over the range of 80–200°C. The gauge length was 20.0 mm and the width of film strips was 2 mm.

Thermogravimetric analysis (TGA) was carried out for the dried precursor polymers and their alternating copolyimides over 50–800°C using a Perkin–Elmer thermal gravimetric analyzer (Model TGA7). During the measurement, dry nitrogen gas was purged at a flow rate of 100 ml/min and a ramping rate of 5.0 K/min was employed.

Residual stress measurements were carried out using a residual stress analyzer equipped with He–Ne laser (632.8 nm wavelength), hot stage, and personal computer, which was made in our laboratory [18,22,23]. For all the Si wafers used, their curvatures were measured before the deposition of polymer films. For each Si wafer deposited with a PAEI precursor film, the variation of its curvature was in-situ monitored as a function of temperature during thermal imidization and subsequent cooling. Here, the imidization was performed by a four-step protocol: 150°C/30 min, 230°C/30 min, 300°C/30 min and 400°C/30 min at a ramping rate of 2.0 K/min. After imidization, the sample was cooled at a cooling rate of 2.0 K/min. From the measured curvature variations, the residual stresses were calculated using the film thickness as well as the biaxial modulus and thickness of Si wafer as reported previously in the literature [18,22,23].

3. Results and discussion

3.1. Structure

PAEI precursors in films were investigated by X-ray diffraction. The X-ray diffraction measurement was carried out in both transmission and reflection modes. The transmission run in which the diffraction vector is in the film plane can provide structural information on the film plane, while the reflection run in which the diffraction vector is in the direction normal to the film plane can give structural information on the direction of film thickness. The measured X-ray diffraction patterns are illustrated in Fig. 2 and their analyses are summarized in Table 1.

The PDPM–6FDA PAEI in films exhibited several diffraction peaks over 4–60° (2θ). The transmission and reflection patterns resemble each other. This indicates that in the film, the precursor polymer chains are aligned randomly rather than in the film plane. The diffraction peak 1 has a *d*-spacing of 11.2–12.1 Å and a coherence length (L_C) of 30–32 Å, depending upon the transmission and reflection patterns. And, the peak 2 reveals a *d*-spacing of 5.70–5.90 Å and a L_C of 24–42 Å, depending upon the transmission and reflection patterns. These peaks may result from the chemical repeat units ordered along the polymer chain axis. According to a previous study [9], poly(*p*-pheneylene pyromellitamic diethyl ester) (PMDA–PDA ES) precursor in films showed a diffraction peak with a *d*-spacing of 10.5 Å (8.4°), which corresponds to the mean length of the chemical repeat unit projected along the polymer chain. This *d*-spacing is comparable to that of the diffraction peak 1 from the PDPM–6FDA PAEI. In fact, the *d*-spacing of 11.2–12.1 Å is approximately equivalent to the average value of the lengths of the PDPM and PD–6FDA units in the chemical repeat unit, which are projected along the polymer chain axis. Considering these results, the diffraction peak 1 in the PDPM–6FDA PAEI is speculated to be a second-order diffraction arising from the chemical repeat units projected along the polymer chain. The *d*-spacing of peak 2 is approximately half of that of peak 1. From the results, it is suggested that peak 2 is the fourth-order diffraction from the molecular ordering along the

Table 1
d-Spacings and coherence lengths (L_C's) of diffraction peaks in the reflection and transmission patterns from poly(amic diisopropyl ester-*alt*-imide)s (PAEIs) in films

Diffraction peak	PDPM–6FDA PAEI	MDPM–6FDA PAEI	MDPM–DSDA PAEI
Transmission pattern			
Peak 1			
Position (2θ)[a]	7.87	8.11	8.15
d-spacing (Å)[b]	11.22	10.89	10.84
Coherence length (Å)[c]	32	28	21
Peak 2			
Position (2θ)	15.01	14.25	14.43
d-spacing (Å)	5.90	6.21	6.13
Coherence length (Å)	42	20	18
Peak 3 (amorphous halo)			
Position (2θ)	16.53	17.72	19.24
d-spacing (Å)	5.36	5.00	4.61
Coherence length (Å)	9	10	10
Peak 4			
Position (2θ)	26.39	25.34	26.27
d-spacing (Å)	3.37	3.51	3.39
Coherence length (Å)	13	16	15
Reflection pattern			
Peak 1			
Position (2θ)	7.30	6.98	7.44
d-spacing (Å)	12.09	12.65	11.88
Coherence length (Å)	30	20	15
Peak 2			
Position (2θ)	15.52	14.31	14.74
d-spacing (Å)	5.70	6.18	6.00
Coherence length (Å)	24	24	15
Peak 3 (amorphous halo)			
Position (2θ)	17.71	17.74	20.14
d-spacing (Å)	5.00	4.99	4.40
Coherence length (Å)	8	9	8
Peak 4			
Position (2θ)	25.85	25.68	26.76
d-spacing (Å)	3.44	3.47	3.33
Coherence length (Å)	12	15	12

[a] Diffraction angle at which the peak is centered.
[b] Calculated from the diffraction angle using the Bragg equation.
[c] Estimated from the full-width at half-maximum of diffraction peak with an instrumental broadening of 0.15° using the Scherrer equation.

chain axis. This molecular ordering has a coherence length of 24–42 Å along the chain axis, depending upon the measurement directions in the film.

Peak 3 is considered to be an amorphous halo. From this peak the mean interchain distance is estimated to be 5.00–5.36 Å. The transmission pattern gave a slightly larger value of the mean interchain distance than the reflection pattern, indicating that the precursor polymer chains are packed more densely in the direction of film thickness than in the film plane. Peak 4 is speculated to arise from the intermolecular packing. The other peaks at $>35°$ may also relate to the interchain packing. The intermolecular packing has a coherence length of 8–13 Å along the lateral direction. However, the intermolecular packing is not in a regular, ordered way.

Similar X-ray patterns were observed for the other precursors in films. The results are compared with those of the PDPM–6FDA PAEI in Fig. 2 and Table 1. For each diffraction peak, the *d*-spacing and coherence length vary with the diffraction measurement modes as observed for the PDPM–6FDA PAEI. The *d*-spacings of peak 1 and peak 2 in these precursor polymers are comparable with those of peak 1 and peak 2 from the PDPM–6FDA PAEI, respectively. These results indicate that all the precursor polymers have almost the same mean length of the chemical repeats, which are projected along the polymer chain axis. However, the coherence length of the polymer ordering along the chain axis is dependent upon the precursor polymer system: the L_C is in the decreasing order of PDPM–6FDA PAEI > MDPM–6FDA PAEI > MDPM–DSDA PAEI. In contrast, the lateral packing order of precursor polymer chains is slightly better in MDPM–6FDA PAEI and MDPM–DSDA PAEI than in PDPM–6FDA PAEI. For the amorphous halo (peak 3), the *d*-spacing is in the decreasing order of PDPM–6FDA PAEI > MDPM–6FDA PAEI > MDPM–DSDA PAEI, while the L_C is in the

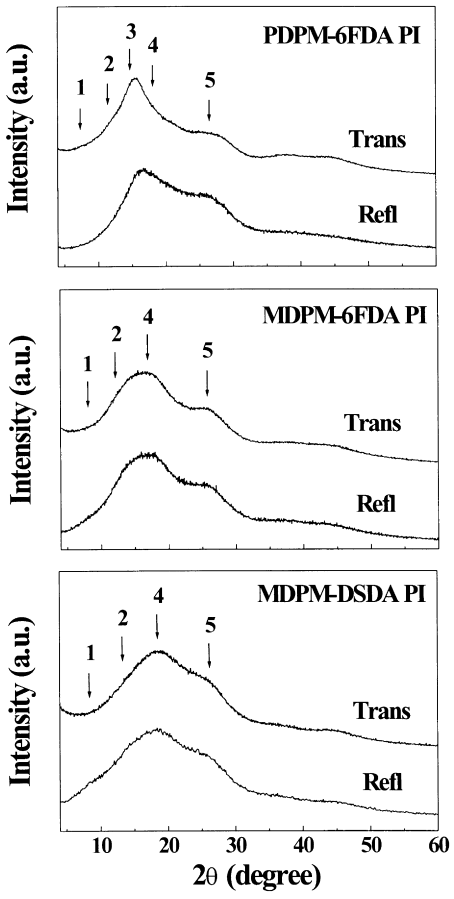

Fig. 3. Reflection and transmission X-ray diffraction patterns of three alternating polyimides in films.

increasing order of PDPM–6FDA PAEI < MDPM–6FDA PAEI ≈ MDPM–DSDA PAEI.

In conclusion, all the precursor films consists of ordered and disordered phases. The ordered phase is estimated to have a dimension of 15–42 Å (along the chain axis) and 8–16 Å (along the lateral direction), depending upon the precursor system. However, the polymer chains even in the ordered phases are not packed in a regular way. And, the overall crystallinity seems to be relatively low.

The precursor polymers in films were thermally imidized at 380°C, and characterized by X-ray diffraction. The measured X-ray patterns are shown in Fig. 3 and the analyzed results are presented in Table 2. For the PDPM–6FDA PI, peak 1 appears in the transmission pattern but its intensity is very weak. Its *d*-spacing and L_C are estimated to be 11.27 and 31 Å, respectively. These are comparable to those of peak 1 for the precursor film. Peak 2 also appears to be very weak: *d*-spacing of 6.97 Å and L_C of 21 Å. However, peak 3 shows strong intensity: *d*-spacing of 5.71 Å and L_C of 28 Å. These peaks are considered to arise from the molecular ordering along the chain axis as observed for the precursor film. In addition, it is noted here that the peaks 1 and 2 do not appear in the reflection pattern and peak 3 appears in the reflection pattern but is relatively weak and broad. These results indicate that the polyimide chains are aligned favorably in the film plane rather randomly but the degree of molecular in-plane orientation is relatively low.

The diffraction peak 4 is an amorphous halo. The amorphous halo has a relatively smaller *d*-spacing than that of the precursor polymer. However, its coherence length is still comparable to that of the precursor polymer film. The *d*-spacing is slightly smaller in the reflection pattern than in the transmission pattern. These results inform us two things. First, the alternating copolyimide chains are packed more densely than their precursor polymer chains. Second, the copolyimide chains are packed more densely in the direction of film thickness than in the film plane as observed for the precursor polymer chains in films. In addition, peak 5, as well as the peaks at >35° are considered to arise from the lateral packing of copolyimide chains.

The other copolyimides in films revealed similar X-ray diffraction patterns as observed for the PDPM–6FDA PI film(Fig. 3). However, peak 3, which corresponds to the peak 3 for the PDPM–6FDA PI film, was not detected for both the MDPM–6FDA PI film and the MDPM–DSDA PI films. This is possibly an indication that the molecular ordering along the polymer chain axis in both the MDPM–6FDA PI film and the MDPM–DSDA PI film is relatively poor when compared to that of the PDPM–6FDA PI film. This may be attributed to the kinked MDPM units on the polymer backbone in both the copolyimides. For both the copolyimide films, the molecular ordering in the lateral direction is, however, comparable to that of the PDPM–6FDA PI film (Table 2). The mean interchain distance increases in the order of MDPM–DSDA PI < PDPM–6FDA PI < MDPM–6FDA PI.

The WAXD results indicate that all the copolyimides form ordered and disordered phases in the film as detected for their precursor polymer films. The ordered phase is estimated to have a dimension of 19–31 Å (along the chain axis) and 8–16 Å (along the lateral direction), depending upon the copolyimides. However, even in the ordered phase the copolyimide chains are packed in an irregular way. And, the overall crystallinity is estimated to be still very low for all the copolyimide films. These results might be attributed mainly to the bend or kinked units, such as MDPM, 6FDA and DSDA, on the polymer backbones.

3.2. Optical and dielectric properties

For the PAEI films and their copolyimide films, refractive indices were measured at an optical frequency of 474.08 THz (i.e. 632.8 nm). In particular, in-plane and out-of-plane refractive indices, n_{xy} and n_z were measured at room temperature, and bulk refractive index (namely, averaged refractive index n_{av}) was estimated from them. The results are summarized in Table 3.

The PAEI films exhibited 1.588–1.621 n_{xy}, 1.563–1.609 n_z and 1.583–1.617 n_{av}, depending on the polymer backbone

Table 2
d-Spacings and coherence lengths (L_C's) of diffraction peaks in the reflection and transmission patterns from alternating copolyimides (PIs) in films

Diffraction peak	PDPM–6FDA PI	MDPM–6FDA PI	MDPM–DSDA PI
Transmission pattern			
Peak 1			
Position (2θ)[a]	7.84	–[b]	–
d-spacing (Å)[c]	11.27	–	–
Coherence length (Å)[d]	31	–	–
Peak 2			
Position (2θ)	12.69	12.85	12.86
d-spacing (Å)	6.97	6.88	6.88
Coherence length (Å)	21	24	19
Peak 3			
Position (2θ)	15.50	–	–
d-spacing (Å)	5.71		–
Coherence length (Å)	28	–	–
Peak 4 (amorphous halo)			
Position (2θ)	17.58	16.80	18.81
d-spacing (Å)	5.04	5.27	4.71
Coherence length (Å)	8	9	9
Peak 5			
Position (2θ)	27.56	26.80	26.32
d-spacing (Å)	3.23	3.42	3.38
Coherence length (Å)	15	16	14
Reflection pattern			
Peak 1			
Position (2θ)	–	7.90	8.81
d-spacing (Å)	–	11.18	10.03
Coherence length (Å)	–	22	19
Peak 2			
Position (2θ)	–	13.06	13.80
d-spacing (Å)	–	6.77	6.41
Coherence length (Å)	–	24	26
Peak 3			
Position (2θ)	15.83	–	–
d-spacing (Å)	5.59	–	–
Coherence length (Å)	21	–	–
Peak 4 (amorphous halo)			
Position (2θ)	18.23	17.09	18.39
d-spacing (Å)	4.86	5.18	4.82
Coherence length (Å)	8	9	8
Peak 5			
Position (2θ)	26.59	26.02	26.25
d-spacing (Å)	3.35	3.42	3.39
Coherence length (Å)	12	13	14

[a] Diffraction angle at which the peak is centered.
[b] Diffraction peak did not appear.
[c] Calculated from the diffraction angle using the Bragg equation.
[d] Estimated from the full-width at half-maximum of diffraction peak with an instrumental broadening of 0.15° using the Scherrer equation.

chemistry and morphological structure. The MDPM–DSDA PAEI film has a relatively high refractive index than the PDPM–6FDA PAEI and MDPM–6FDA PAEI films while the MDPM–6FDA PAEI film shows a lower refractive index than the PDPM–6FDA PAEI film. These results indicate that: first, the refractive indices are reduced by incorporating fluorine atoms, which have the smallest polarizability, into the polymer backbone and second, the incorporation of bend or kinked units, such as the MDPM unit, into the polymer backbone causes a loosening of the interchain packing, consequently resulting in a reduction in the refractive indices.

The out-of-plane birefringence ($\Delta = n_{xy} - n_z$), which is a measure of chain in-plane orientation, was 0.012–0.037, depending on the precursor polymers. The Δ is in the increasing order of MDPM–DSDA PAEI < MDPM–6FDA PAEI < PDPM–6FDA PAEI. However, all the precursor films have relatively low Δs, indicating that the in-plane orientations of the precursor chains in the films are relatively very low. These results are consistent with the WAXD results described in the earlier part.

The copolyimides in films showed relatively higher refractive indices than their precursors: depending on the

Table 3
Optical and dielectric properties of poly(amic diisopropyl ester-*alt*-imide) (PAEI) films and their alternating copolyimide (PI) films

Polymer	Optical properties[a]				Dielectric properties[b]			
	n_{xy}	n_z	n_{av}	Δn	ϵ_{xy}	ϵ_z	ϵ_{av}	$\Delta\epsilon$
PAEI precursor film[c]								
PDPM–6FDA PAEI	1.600	1.563	1.587	0.037	2.560	2.443	2.521	0.127
MDPM–6FDA PAEI	1.588	1.573	1.583	0.015	2.522	2.474	2.506	0.048
MDPM–DSDA PAEI	1.621	1.609	1.617	0.012	2.628	2.589	2.615	0.039
Alternating copolyimide film[d]								
PDPM–6FDA PI	1.644	1.593	1.627	0.051	2.703	2.538	2.648	0.165
MDPM–6FDA PI	1.618	1.602	1.613	0.016	2.618	2.566	2.601	0.052
MDPM–DSDA PI	1.682	1.678	1.681	0.004	2.829	2.816	2.825	0.013

[a] Measured at 632.8 nm (474.08 THz).
[b] Estimated from refractive indices using the Maxwell equation ($\epsilon = n^2$).
[c] Film thickness was ca. 5 μm.
[d] Film thickness was ca. 4 μm.

copolyimide backbone chemistry, the n_{xy} was 1.618–1.682, the n_z 1.593–1.678 and the n_{av} 1.613–1.681. These high refractive indices in the copolyimide films might result mainly from the morphological structures densified through thermal imidization. The PDPM–6FDA PI film exhibited a larger Δ than its precursor film, whereas the MDPM–DSDA PI showed a smaller Δ than its precursor film. However, the MDPM–6FDA PI revealed a Δ that is comparable to that of its precursor film.

Dielectric constants were estimated from the measured refractive indices using the Maxwell equation [24]: $\epsilon = n^2$ where ϵ is the dielectric constant. Overall, all the precursors and the resultant copolyimides exhibited relatively low dielectric constants as shown in Table 3. The PDPM–6FDA PI showed a relatively large dielectric anisotropy, whereas the other PIs revealed small dielectric anisotropies. All the copolyimides are good candidate dielectrics for the fabrication of microelectronic devices. Regarding dielectric constants and anisotropies, the MDPM–6FDA PI is, however, relatively better than the other PIs.

3.3. Thermal stability and imidization-induced shrinkage behavior

Fig. 4 shows TGA thermograms measured for the precursor polymers in films. In heating run, the PAEI precursor polymer was thermally stable up to 230–263°C, depending upon the backbone structures. All the precursor polymers began to imidize in the range of 230–263°C, and their imidizations were completed around 330°C. The onset temperatures of imidization (T_i) are relatively higher than those measured previously for aromatic poly(amic diethyl ester)s and poly(amic dimethyl ester)s [7,25]. The high T_i in the PAEI precursors may relate to the relatively high chain rigidity owing to the PD–6FDA and MD–DSDA imide segments on the polymer backbones. The thermal imidization behaviors have been investigated further by means of ODSC, which are discussed in the next section.

Thermal imidization brought a weight loss of ca. 13%, which corresponds to the isopropyl alcohol byproduct removed from the precursor polymer. Theoretically, both the PDPM–6FDA PAEI and the MDPM–6FDA PAEI have a weight loss of 13% through thermal imidization. And, the MDPM–DSDA PAEI has a weight loss of 14.3% via thermal imidization. In comparison, there is expected a 23% weight loss for the thermal imidizations of both PDPM–6FDA and MDPM–6FDA copoly(amic diisopropyl ester)s and a 25% weight loss for the thermal imidization of MDPM–DSDA copoly(amic diisopropyl ester). According to a previous study, poly(amic acid) is known to generally contain about two NMP molecules per chemical repeat unit which have two amic acid groups via the complexation of amic acid group and NMP. Thus, both PDPM–6FDA and MDPM–6FDA copoly(amic acid)s, which have four amic acid groups per chemical repeat unit, are expected to have a weight loss of 36.7% via thermal imidization. And, the MDPM–DSDA copoly(amic acid) may have a weight loss of 39.4% through imidization. The PAEI precursors prepared in the present study have relatively low weight losses because of thermal imidization because they already contain imide segments of 50 mol% on the backbone. These low weight losses are reflected directly

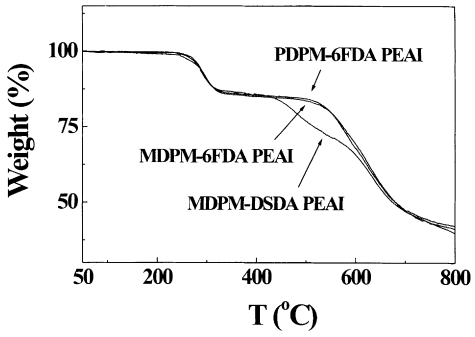

Fig. 4. Thermogravimetric thermograms of poly(amic diisopropyl ester-*alt*-imide)s and their alternating copolyimides in films.

on the shrinkage generated during imidization, consequently leading to a low degree of shrinkage in the formation of alternating copolyimides.

In the heating runs, the imidized copolyimides were continuously heated further up to 800°C (Fig. 4). The MDPM–DSDA PI exhibited a two-step degradation: the first-step degradation began at ca. 418°C and the second-step degradation started at ca. 570°C. In contrast, both the PDPM–6FDA PI and the MDPM–6FDA PI began to degrade at ca. 522°C in a single-step manner. On the polymer backbone, the MDPM–6FDA PI consists of MDPM and MD–6FDA units per chemical repeat on the backbone, while the MDPM–DSDA PI has MDPM and MD–DSDA units per chemical repeat on the backbone. In comparison, the MD–6FDA unit provides a relatively higher thermal stability to the copolyimide than the MD–DSDA unit. Therefore, the first-step degradation in the MDPM–DSDA PI may be attributed to the degradation of MD–DSDA units on the polymer backbone. In conclusion, the thermal stability is in the increasing order of MDPM–DSDA PI < MDPM–6FDA PI ≈ PDPM–6FDA PI.

3.4. Glass transition and imidization behavior

For the PAEI precursor polymers, glass transition and imidization behaviors were examined by ODSC. The measured ODSC thermograms were nicely separated into two parts, specific heat flow and kinetic heat flow, in accordance to the method reported previously elsewhere [9,11,15]. The separated specific and kinetic heat flow thermograms are shown in Fig. 5.

The PDPM–6FDA PAEI precursor films revealed two transitions in the specific heat flow profile: one at 137.8°C and the other at 251.5°C. Here, the transition at 137.8°C is relatively weaker than that at 251.5°C. According to an ODSC study reported previously [9], aromatic poly(amic dialkyl ester) precursors in films exhibited their glass transition temperatures (T_g) in the range of 201–235°C, depending on the precursor chain rigidity: poly(*p*-phenylene biphenyltetracarboxamic diethyl ester), poly(*p*-phenylene biphenyltetracarboxamic dimethyl ester), poly(4,4′-oxydiphenylene biphenyltetracarboxamic diethyl ester), poly(*p*-phenylene pyromellitamic diethyl ester) and poly(4,4′-diphenylene pyromellitamic diethyl ester). And, aromatic poly(amic acid) precursors, solvent free, were previously estimated to have T_g in the range of 166–284°C, depending on the precursor chain rigidity [11,15]: poly(*p*-phenylene biphenyltetracarboxamic acid), poly(4,4′-oxydiphenylene biphenyltetracarboxamic acid), poly(*p*-phenylene pyromellitamic acid), poly(4,4′-diphenylene pyromellitamic acid), poly(*p*-phenylene benzophenonetetracarboxamic acid) and poly(4,4′-oxydiphenylene 3,3′-oxydiphthalamic acid). Considering the T_gs of aromatic polyimide precursors in literature, the transition at 251.5°C is accounted to result from the glass transition of the PDPM–6FDA PAEI precursor film. However, another transition appeared at 137.8°C, which is much lower than the T_g, so that this transition is not fully understood.

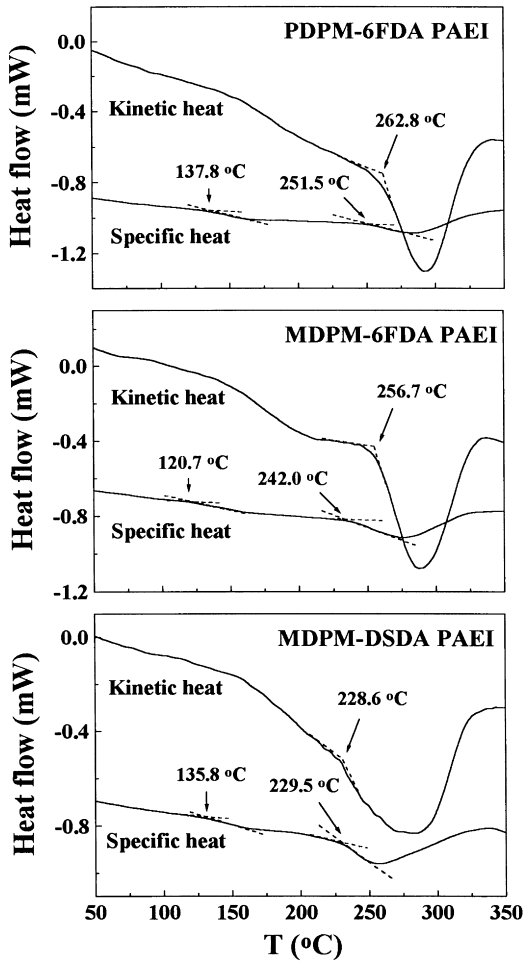

Fig. 5. Oscillating DSC thermograms of poly(amic diisopropyl ester-*alt*-imide)s in films.

In addition information was obtained about the thermal imidization of PDPM–6FDA PAEI precursor from the separated kinetic heat flow profile. In the heating run, the precursor polymer started to imidize at 262.8°C and the imidization continued until 343°C: here, the T_i is estimated to be 262.8°C. This thermal imidization behavior is consistent with the TGA thermogram which was qualitatively described earlier.

Similar ODSC thermograms were obtained for the other PAEI precursor polymers (Fig. 5). The T_g and T_i were estimated to be 242.0 and 256.7°C for MDPM–6FDA PAEI, and 229.5°C and 228.6°C for MDPM–DSDA PAEI, respectively. The low temperature transitions have also been measured for these precursors but are fully not understood either.

The T_g in a polymer is generally known to be primarily dependent upon the polymer chain rigidity: higher chain rigidity exhibits a higher T_g. Thus, the measured T_g data suggest that the chain rigidity in the PAEI precursor polymer is in the increasing order of MDPM–DSDA

Table 4
Thermal properties poly(amic diisopropyl ester-*alt*-imide) (PAEI) films and their alternating copolyimide (PI) films

Polymer film	PAEI precursor				Alternating copolyimide (PI)			
	T_g[a] (°C)	T_i[b] (°C)	TEC[c] (ppm/°C)	Stress[d] (MPa)	T_g[e] (°C)	T_d[f] (°C)	TEC[g] (ppm/°C)	Stress[h] (MPa)
PDPM–6FDA	251.5	262.8	35	19	≥ 400	29	522	46
MDPM–6FDA	242.0	256.7	47	53	370	43	522	76
MDPM–DSDA	229.5	228.6	48	24	385	40	418	64

[a] Glass transition temperature meeasured by ODSC.
[b] The onset temperature of imidization measured by ODSC.
[c] In-plane TECs were measured by TMA, and averaged over 80–140°C.
[d] Residual stress of PAEI film measured at 30°C by residual stress analysis.
[e] Glass transition temperature measured by residual stress analysis.
[f] Degradation temperature measured by TGA.
[g] In-plane TECs were measured by TMA, and averaged over 100–200°C.
[h] Residual stress of PI film measured at 30°C by residual stress analysis.

PAEI < MDPM–6FDA PAEI < PDPM–6FDA PAEI. In comparison, the MDPM unit seems to make a relatively higher degree of kink on the polymer backbone than the PDPM unit. The DSDA unit gives a relatively higher flexibility on the polymer backbone than the 6FDA unit. The chain rigidities in the precursor polymers were observed to influence their imidization behaviors: a precursor polymer with higher chain rigidity was imidized at a higher temperature. For all the PAEI precursor polymers, their T_is are very close to or higher than their T_gs. This suggests that for the PAEI precursors, the imidization requires chain mobility in a certain level.

3.5. Thermal expansion and residual stress behavior

In-plane TECs were measured by TMA. For each precursor polymer film, the measured TECs were averaged over 80–140°C, which is far below its T_i. For each alternating copolyimide film, the measured TECs were averaged over 100–200°C. The TEC results are summarized in Table 4. The precursor films exhibited a TEC of 35–48 ppm/°C, depending upon the type of precursor polymers: the TEC increases in the order of PDPM–6FDA PAEI < MDPM–6FDA PAEI ≈ MDPM–DSDA PAEI. The resultant copolyimide films revealed a TEC of 29–43 ppm/°C, depending on the type of copolyimides: the TEC increases in the order of PDPM–6FDA PI < MDPM–DSDA PI < MDPM–6FDA PI. In comparison, all the PAEI precursors in films show relatively larger TECs than their copolyimides. The relatively low TECs of copolyimides might result from their relatively high chain rigidity and dense chain packing, compared to those of the precursor polymers, as discussed earlier in Section 3.1.

In general, the TEC in a polymer film, adhered to a substrate, is known to relate directly to the residual stress which is critical to the stability of the polymer/substrate [10,20,22,23,26,27]. The residual stress at the interface is caused by the mismatching between TECs of the polymer and substrate: higher mismatching of TECs generates higher residual stress at the interface. For this reason, the residual stresses in the precursor films and resultant copolyimide films were in-situ measured on silicon wafers primed with a silane coupling agent during thermal imidization and subsequent cooling. The measured residual stress–temperature profiles are illustrated in Fig. 6.

The PDPM–6FDA PAEI film exhibited a residual stress of 19 MPa at 30°C. In the heating run with a four-step protocol described in Section 2, the residual stress was decreased gradually with temperature but was influenced by the heating steps. In particular, the stress was built up during soaking at the first step (150°C): the stress at 150°C was increased to 15 MPa from 11 MPa during soaking. This stress development might be due to densification of polymer film in the direction of film thickness by removal of residual solvent and possibly partial imidization even though the removal of residual solvent and the partial imidization are involved in a very small amount. Such stress development was detected during soakings at the other heating steps but the developed stresses were relatively very small. Overall, the stress generated in the polymer film/substrate interface was relaxed with increasing temperature. This stress relaxation might be attributed to the enhancement of chain mobility in the polymer film by heating, regardless of the imidization conversion in the precursor film.

The imidized PDPM–6FDA film revealed a residual stress of 2 MPa at 400°C. In the cooling run, the stress increased linearly with decreasing temperature and finally reached 46 MPa at 30°C. In general, the residual stress in a polymer adhered on a substrate is always built up below T_g of the polymer but is relaxed out above T_g, because of the dependency of polymer chain mobility on T_g [10,20,22,23,26,27]. Therefore, the T_g can be estimated to be 400°C or slightly higher than 400°C from the stress–temperature profile measured during the cooling run.

Similar stress–temperature profiles were measured for the MDPM–6FDA PAEI and MDPM–DSDA PAEI films on silicon wafers (Fig. 6). In the heating runs, their stresses decreased gradually with elevating temperature in a similar

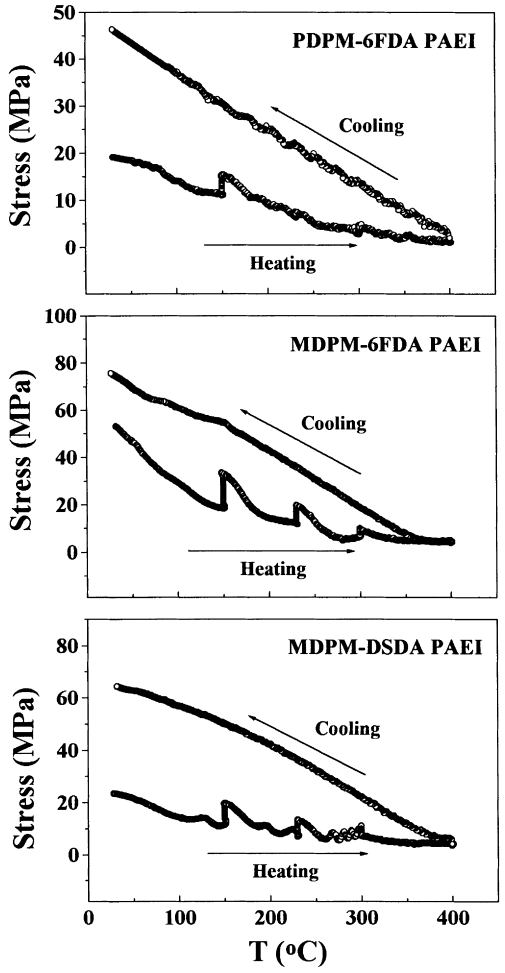

Fig. 6. Residual stress variations of poly(amic diisopropyl ester-*alt*-imide)s and their alternating copolyimides in films adhered on silicon wafers as a function of temperature, which were in-situ measured during thermal imidization and subsequent cooling.

manner as revealed by the PDPM–6FDA PAEI film. However, the stress developments during soaking at each heating step appeared distinctively. The MDPM–6FDA PAEI film showed a stress of 53 MPa. The imidized film exhibited 4.5 MPa at 400°C. In the cooling run, the stress stayed at the level of 4.5 MPa until 370°C and then increased almost linearly with decreasing temperature, finally reaching 76 MPa at 30°C. From this stress–temperature profile, the MDPM–6FDA PI is estimated to have a T_g of 370°C. The MDPM–DSDA PAEI film revealed 23 MPa stress at 30°C. The imdized film had a stress of 4 MPa at 400°C and the stress level retained until 385°C in the cooling run, indicating that the copolyimide has a glass transition at 385°C. However, the stress was built up almost linearly by decreasing temperature and reached 64 MPa at 30°C.

The residual stress of the PAEI precursor film adhered on the silicon substrate is in the increasing order of PDPM–6FDA PAEI < MDPM–DSDA PAEI < MDPM–6FDA PAEI. The residual stress in a spin-cast polymer film is sensitive to the amount of residual solvent and mechanical properties in addition to the TEC [10,20,22,23,26,27]. In particular, the residual solvent is known to affect the film stress severely: the residual stress is suppressed highly with increasing the amount of residual solvent. Thus, the relatively low stress in the PDPM–6FDA PAEI and MDPM–DSDA PAEI films might be due to the relatively large amount of residual solvent in the films. For the imidized films, the stress at 30°C increases in the order of PDPM–6FDA PI < MDPM–DSDA PI < MDPM–6FDA PI. Here, the measured residual stress, an in-plane property, varies with the aforementioned TEC and mechanical properties, which are also in-plane properties. These properties are dependent further on the rigidity and in-plane orientation of the polymer chain. In general, higher chain rigidity gives lower residual stress and lower TEC. The lower residual stress and lower TEC are also provided by higher chain in-plane orientation. However, the degree of chain in-plane orientation is relatively very small for all the alternating copolyimides studied here. Therefore, these stress results together with the measured TECs and T_gs suggest that the chain rigidity of alternating copolyimide is in the increasing order of MDPM–6FDA PI < MDPM–DSDA PI < PDPM–6FDA PI.

4. Conclusions

Three poly(amic diisopropyl ester-*alt*-imide)s, which are a new type of polyimide precursors, were synthesized. The precursors consist of amic ester and imide units on the backbone, so that they are hydrolytically stable as well as less shrinkable through thermal imidization. These precursors are soluble in common solvents, such as NMP, DMAc and DMF, which are widely used as good solvents for most polyimide precursors: namely, all the precursor polymers have an easy processability.

All the precursors and the resultant alternating copolyimides in films were measured to consist of ordered and disordered phases. The ordered phases are estimated to have a dimension of 15–42 Å (along the chain axis) and 8–16 Å (along the lateral direction), depending upon the precursors and their copolyimides. However, the polymer chains in the ordered phases are packed in an irregular way, regardless of the precursors and resultant copolyimides. The overall crystallinity is relatively low for all the precursors and resultant copolyimides in films. These results might be attributed mainly to the bend or kinked units, such as MDPM, 6FDA and DSDA, on the polymer backbones.

In addition, properties of these precursor polymers and their polyimides in films: optical and dielectric properties, glass transition, thermal imidization characteristics, thermal stability, thermal expansion and residual stress were investigated in detail. In conclusion, the precursor polymers, as well as the resultant alternating copolyimides have

properties suitable for applications in the fabrication of microelectronic devices.

Acknowledgements

This study was supported in part by the Ministry of Education Korea (the New Materials Research Fund in 1998 and the Basic Science Research Institute Program-BSRI-98-3438) and by the Korea Science and Engineering Foundation (KOSEF) (Contract Nos. 95-0501-08-01-3 and 961-0301-006-2).

References

[1] Ghosh KL, Mittal KL, editors. Polyimides-fundamentals and applications New York: Dekker, 1996.
[2] Sroog CE. Prog Polym Sci 1991;16:561.
[3] Czornyj G, Chen KJ, Prada-Silva G, Arnold A, Souleotis HA, Kim S, Ree M, Volksen W, Dawson D, DiPietro R. IEEE proceedings of electrical and computer technology, 42. 1992. p. 682.
[4] Deutsch A, Swaminathan M, Ree M, Surovic C, Arjavalingam G, Prasad K, McHerron DC, McAllister M, Kopcsay GV, Giri AP. IEEE Trans Compt Packaging and Manufacture Technol, Part B: Adv Packaging 1994;17:486.
[5] Ree M, Yoon DY, Volksen W. J Polym Sci, Part B: Polym Phys Ed 1991;29:1203.
[6] Kreuz JA, Endrey AL, Gay FP, Sroog CE. J Polym Sci, Part A-1 1966;4:2607.
[7] Kim K, Ryou JH, Kim Y, Ree M, Chang T. Polym Bull 1995;34:219.
[8] Kim Y, Ree M, Chang T, Ha CS, Nunes TL, Lin JS. J Polym Sci, Part B: Polym Phys Ed 1995;33:2075.
[9] Kim SI, Shin TJ, Ree M. Polymer 1999;40:2263.
[10] Ree M, Nunes TL, Czornyj G, Volksen W. Polymer 1992;33:1228.
[11] Kim SI, Pyo SM, Kim K, Ree M. Polymer 1998;39:6489.
[12] Ree M. Unpublished results.
[13] Rhee SB, Park JW, Moon BS, Chang JY. Macromolecules 1993;26:404.
[14] Ree M, Goh WH, Park JW, Lee MH, Rhee SB. Polym Bull 1995;35:129.
[15] Kim SI, Pyo SM, Ree M. Macromolecules 1997;30:7890.
[16] Ree M, Nunes TL, Lin JS. Polymer 1994;35:1148.
[17] Manual book of data analysis, Tokyo: Rigaku Corporation, 1997 Japan.
[18] Ree M, Kim K, Woo SH, Chang H. J Appl Phys 1997;81:698.
[19] Scherrer S. Nachr Gottinger Gesell 1918;2:98.
[20] Ree M, Chu CW, Goldberg MJ. J Appl Phys 1994;75:1410.
[21] Goh WH, Kim K, Ree M. Korea Polym J 1998;6:241.
[22] Ree M, Shin TJ, Park YH, Kim SI, Woo SH, Cho CK, Park CE. J Polym Sci, Part B: Polym Phys 1998;36:1261.
[23] Ree M, Park YH, Kim K, Cho CK, Park CE. Polymer 1997;38:6333.
[24] Maxwell JC. N Philos Trans 1865;155:459.
[25] Ree M, Kim K. Unpublished results.
[26] Lee KW, Viehbeck A, Walker GF, Cohen S, Zucco P, Chen R, Ree M. J Adhes Sci Technol 1996;10:807.
[27] Ree M, Swanson S, Volksen W. Polymer 1993;34:1423.